

# Effect of heat treatment on microstructure and mechanical properties of a new $\beta$ high strength titanium alloy



Zhaoxin Du, Shulong Xiao, Lijuan Xu, Jing Tian, Fantao Kong, Yuyong Chen \*

National Key Laboratory of Science and Technology on Precision Heat Processing of Metals, Harbin Institute of Technology, Harbin 150001, PR China

## ARTICLE INFO

### Article history:

Received 9 July 2013

Accepted 28 September 2013

Available online 8 October 2013

### Keywords:

Microstructure

Mechanical property

High strength titanium alloy

Heat treatment

## ABSTRACT

Microstructure and mechanical properties of a new  $\beta$  high strength Ti–3.5Al–5Mo–6V–3Cr–2Sn–0.5Fe titanium alloy were investigated in this paper. Both the  $\alpha/\beta$  and  $\beta$  solution treatment and subsequent aging at temperatures ranging from 440 °C to 560 °C for 8 h were introduced to investigate the relationship between microstructures and properties. Microstructure observation of  $\alpha/\beta$  solution treatment plus aging condition shows that the grain size is only few microns due to the pinning effect of primary  $\alpha$  phase. The  $\beta$  solution treatment leads to coarser  $\beta$  grain size and the least stable matrix. The size and volume fraction of secondary  $\alpha$  are very sensitive to temperature and strongly affected the strength of the alloy. When solution treated at 775 °C plus aged at 440 °C, the smallest size (0.028  $\mu\text{m}$  in width) of secondary  $\alpha$  and greatest volume fraction (61%) of  $\alpha$  resulted in the highest yield strength (1624 MPa). And the yield strength decreased by an average of 103 MPa with every increase of 40 °C due to the increase of volume fraction and decrease of the size of secondary  $\alpha$ . In  $\beta$  solution treatment plus aging condition, tensile results shows that the strength of the alloy dramatically decreased by an average of 143 MPa for every increase of 40 °C because of larger size of secondary  $\alpha$  phase than  $\alpha/\beta$  solution treated plus aged condition.

© 2013 Elsevier Ltd. All rights reserved.

## 1. Introduction

There is considerable interest in the development of  $\beta$  titanium alloys due to their best combination of high strength and toughness, and offer the highest strength-to-weight ratio of titanium alloys [1,2]. As results of these properties, beta titanium alloys have potential applications in aerospace industries [3–7]. And in recent decades, the application of  $\beta$  titanium alloys increased and possess a reasonable share of market for aerospace applications [8,9].

For  $\beta$  titanium alloys, a high strength can be brought in by precipitation of fine scale  $\alpha$  phase. But they are not used at a very high strength level due to the poor ductility. For example, the forging of the first commercially  $\beta$  titanium alloy Ti–13V–11Cr–3Al, which was developed to used on the SR-71 “Blackbird” reconnaissance airplane, was used at the 1240 MPa strength level but with a minimum elongation of 2%, so it is being replaced there by  $\beta$ -C [10]. Another advanced  $\beta$  titanium alloy Timetal555, which is used for replacement for Ti-10-2-3 and steel components such as large landing-gear forgings and high-strength fasteners, is capable of achieving strengths up to 1517 MPa, but it is not used at this strength level due to the poor ductility [3]. The strength and

ductility of  $\beta$  titanium alloys are strongly dependent on microstructure. The tensile strength could be improved by the precipitation of small secondary  $\alpha$  phase because that the secondary  $\alpha$  phase could act as a barrier to slip propagation and cause a microstructure condition similar to a dispersion strengthened system [11]. The decrease in size or increase in volume fraction of secondary  $\alpha$  phase will improve the strength of  $\beta$  titanium alloys [12]. The morphology of primary  $\alpha$  phase can affect the ductility of  $\beta$  titanium alloys. The work done by Terlinde et al. shows that the alloy with elongated  $\alpha$  exhibits lower ductility compares to the globular shape at the same yield strength level [13]. The presence of grain boundary  $\alpha$  layer will lead to early crack and result in the lower ductility [14]. Generally, the microstructure parameters can be changed to improve the mechanical properties by two step heat treatments of  $\beta$  titanium alloys. The first step is slightly below or above  $\beta$  transus to homogenize matrix and the second is to strengthen the alloy by precipitate of finer  $\alpha$  at lower temperature. It was found that the Ti–6Cr–5Mo–5V–4Al alloy shows a higher strength when solution treated at  $\alpha/\beta$  than in single  $\beta$  field [15]. However, the Ti–10V–2Fe–3Al alloy exhibits an opposite result that the alloy solution treated at single  $\beta$  field (regardless of processing temperature) plus aged results in higher strength than solution treated at  $\alpha/\beta$  field plus aged [9]. Thus, the relationship between microstructure and properties of  $\beta$  titanium alloys is not well known and it is necessary to study deeply during heat treatment.

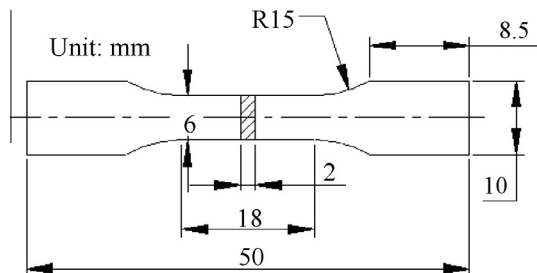
\* Corresponding author. Tel./fax: +86 451 86418802.

E-mail address: [yychen@hit.edu.cn](mailto:yychen@hit.edu.cn) (Y. Chen).

**Table 1**

Chemical composition of Ti–3.5Al–5Mo–6V–3Cr–2Sn–0.5Fe alloy (wt.%).

Element	Al	Mo	V	Cr	Sn	Fe	H	N	O	Ti
Wt.%	3.61	5.26	5.71	2.97	1.91	0.494	0.0045	0.009	0.082	Bal.

**Fig. 1.** Dimensioned schematic of the tensile specimen.

A newly designed  $\beta$  titanium alloy Ti–3.5Al–5Mo–6V–3Cr–2Sn–0.5Fe has been studied in this paper. Solution treated at  $\alpha/\beta$  and  $\beta$  field with different aging temperature were carried out carefully. The microstructural evolution and tensile properties of the alloy during heat treatment were studied to investigate the relationship between microstructures and mechanical properties of the alloy.

## 2. Materials and methods

The investigations were conducted on a new  $\beta$  high strength titanium alloy, which nominal composition is Ti–3.5Al–5Mo–6V–

**Table 2**

Tensile property of the alloy in solution treated condition.

ST (°C)	UTS (MPa)	YS (MPa)	El (%)	RA (%)
775	986	981	22.3	46.8
830	914	908	27.3	56.4

3Cr–2Sn–0.5Fe. The ‘moly equivalent’ (Mo Eq) of the alloy is 11.4 that is calculated by the following equation [8]:

$$\text{Mo Eq} = 1.0\text{Mo} + 0.67\text{V} + 1.6\text{Cr} + 2.9\text{Fe} + \dots - \text{Al} \quad (1)$$

The alloy was melted using double vacuum consumable arc melting process to obtain an original ingot. The chemical composition analysis was performed at top and bottom of the ingot and the average value of compositions were listed in Table 1. The ingot with 200 mm in length and 150 mm in diameter was first forged down to 120 mm in diameter billet with reduction of 83.6% after soaking in the  $\beta$  field at 980 °C for 2 h. The billet was soaked in the  $\alpha/\beta$  field at 760 °C for 1.5 h and then hot rolled at same temperature to a round bars with 80 mm in diameter with reduction of 65.1%. The  $\beta$  transition temperature of the alloy measured by metallographic method is 815 °C  $\pm$  5 °C. Samples from the as forged

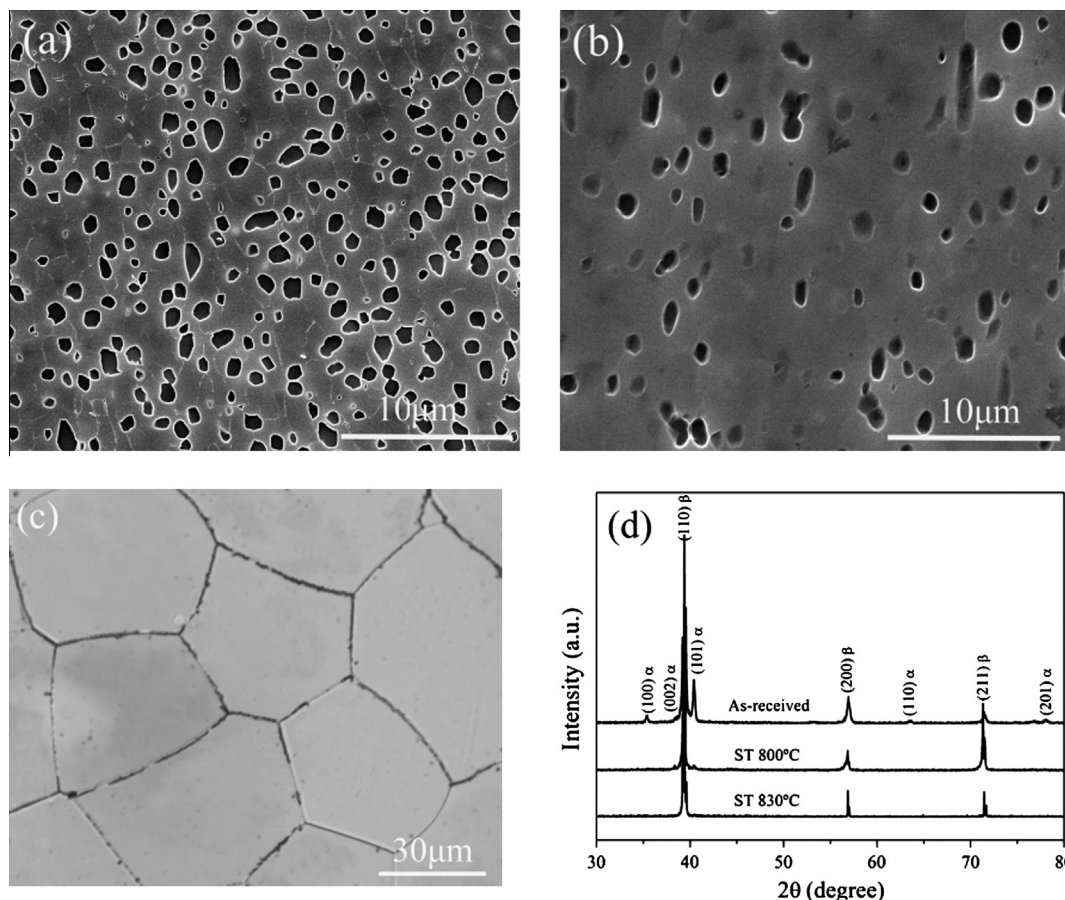


**Fig. 2.** Micrographs of as-received and solution treated alloy along the transversal section and X-ray diffraction spectra: (a) as-received alloy (b) solution treated at 775 °C for 1 h (c) solution treated at 830 °C for 0.5 h (d) X-ray diffraction spectra of samples (a), (b) and (c).

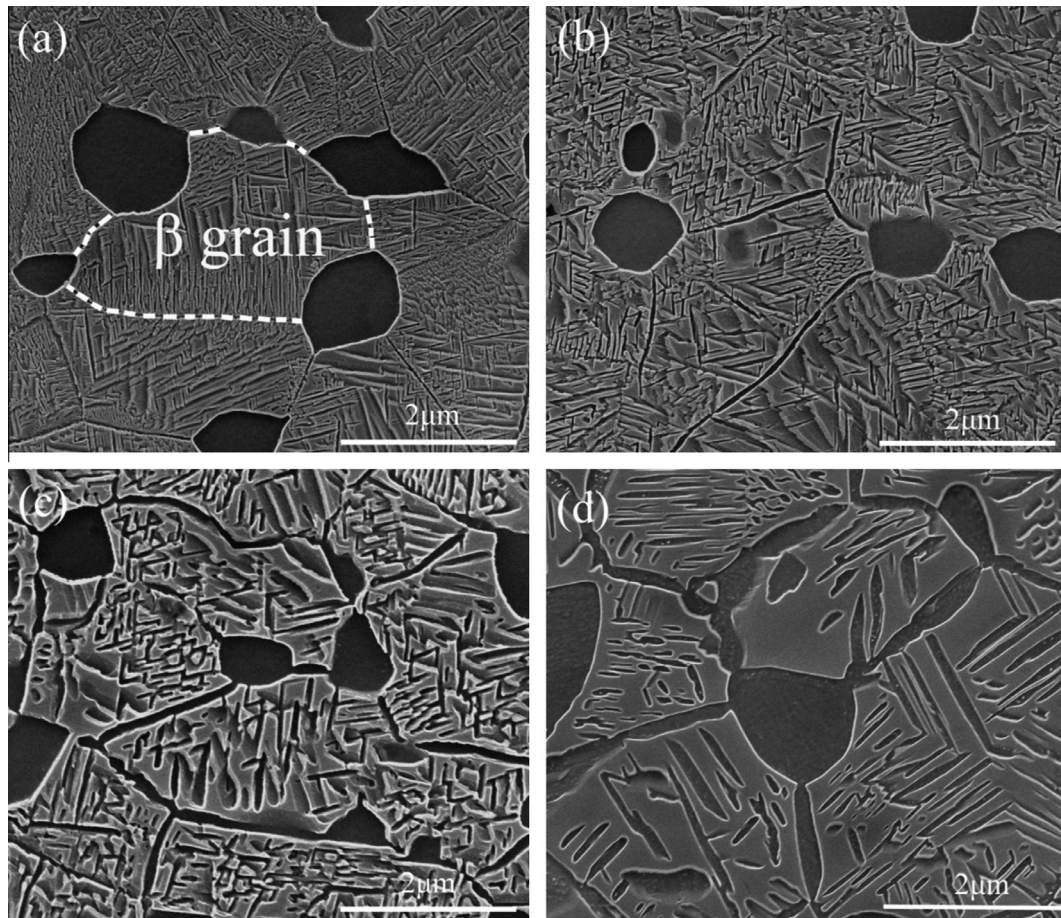


**Fig. 3.** Microstructures of the alloy along the transversal section solution treated at 775 °C plus aged for 8 h at: (a) 440 °C, (b) 480 °C, (c) 520 °C and (d) 560 °C.

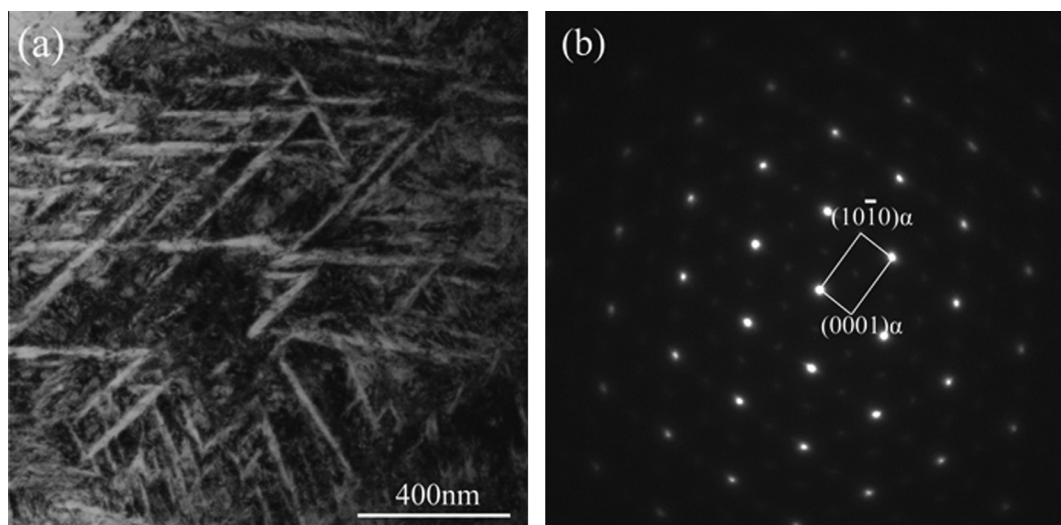


**Fig. 4.** Bright field micrograph of alloy solution treated at 775 °C plus aged at 440 °C for 8 h: (a) acicular  $\alpha$  phase distributing in  $\beta$  matrix, (b) its corresponding selected electron diffraction patterns.

material were firstly solution treated at 775 °C for 1 h and 830 °C for 0.5 h respectively and followed by air cooling. Then, the samples after solution treated were undergone aging heat treatment at 440 °C, 480 °C, 520 °C and 560 °C respectively for 8 h and followed by air cooling.

The microstructural evolution along the transversal section with respect to the rolling direction of rod bar was characterized

by scanning electron microscopy (SEM) and transmission electron microscopy (TEM) techniques. SEM observation was performed on field emission gun scanning electron microscopy Quanta 200FEG. The specimens for SEM observation were polished with 400–2000 grid SiC paper in water, and then etched in the Kroll's reagent (10 ml HF, 30 ml HNO<sub>3</sub> and 200 ml H<sub>2</sub>O). Image analysis software was used to calculate the size and the volume fraction of  $\alpha$  phase



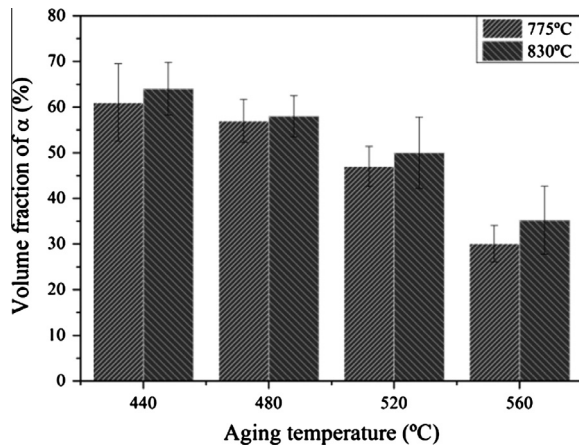


Fig. 5. Volume fraction of  $\alpha$  phase as function of aging temperature.

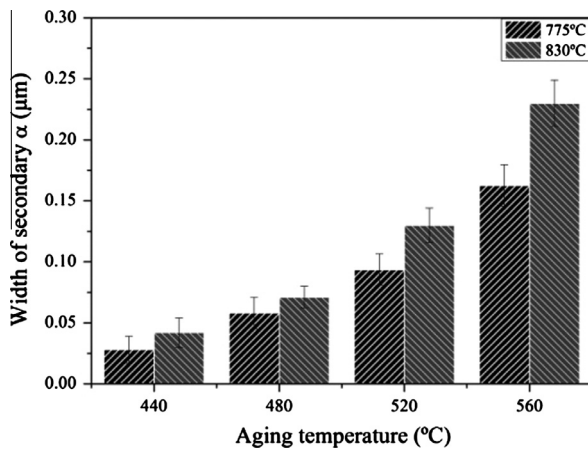


Fig. 6. The width of secondary  $\alpha$  phase as function of aging temperature.

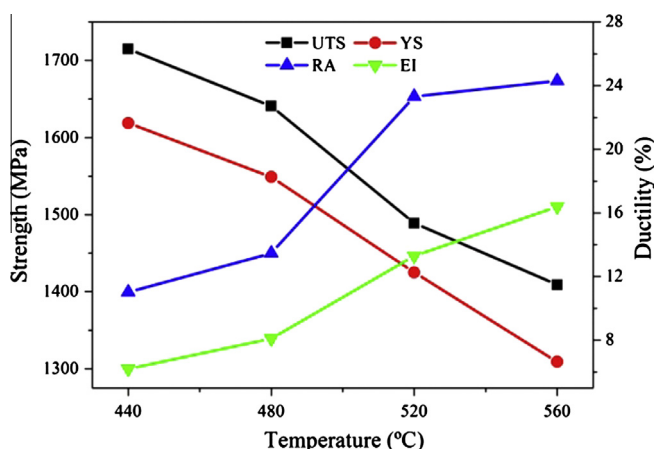


Fig. 7. Tensile properties of the alloy after solution treated at  $\alpha/\beta$  field plus aged.

Flat tensile specimens with dimensions shown in Fig. 1, were performed on Instron 5500R testing machine at room temperature, driven at crosshead speed of 1 mm/min. The specimens were cut from the material with their longitudinal directions parallel to the rolling directions and polished with 400–2000 grid SiC paper in water. In order to ensure repeatability, each value is an average of three measurements. And fracture surfaces were observed by SEM.

### 3. Results

#### 3.1. As forged and solution treated conditions

Fig. 2 shows the microstructures of as forged and solution treated Ti–3.5Al–5Mo–6V–3Cr–2Sn–0.5Fe alloy along the transversal section. As shows in Fig. 2(a), the alloy finally forged at  $\alpha/\beta$  region consists of  $\beta$  microstructure and spherically  $\alpha$  phase (primary  $\alpha$ ). During the deformation process in  $\alpha/\beta$  phase field, a crystallographic texture in the  $\beta$  and  $\alpha$  phase can develop [16]. In  $\beta$  titanium alloys, the recrystallised  $\alpha$  structure can be obtained by processing them at  $T_{\beta}-50^{\circ}\text{C}$  to  $T_{\beta}-100^{\circ}\text{C}$  [17]. Weiss and Ding et al. [18,19] showed that both the low and high angle sub-boundary formed across the  $\alpha$  plates during hot working. Subsequent working provided a driving force enable some beta phase can penetrate into  $\alpha$  phase along sub-boundaries and then lead to the formation of globularization  $\alpha$  [20,21]. In addition, the deformation rate also affect the globularization of  $\alpha$  phase according to the work done by Xu et al. [22] that the globularization will be complete when the deformation amount is higher than 60%.

After solution treated at  $775^{\circ}\text{C}$  for 1 h, the volume fraction of primary  $\alpha$  phases significantly reduced from 20% to 5% (Fig. 2(b)). Fig. 1(d) shows the XRD patterns of the alloy as forged and solution treated. The alloy after solution treated at  $775^{\circ}\text{C}$  shows smaller intensity of  $(002)_{\alpha}$  and  $(101)_{\alpha}$  peaks and the  $(100)_{\alpha}$ ,  $(110)_{\alpha}$  and  $(201)_{\alpha}$  peaks disappeared compared to as-forged material. Solution treated at  $830^{\circ}\text{C}$  resulted in coarse  $\beta$  grains and the mean diameter is about  $58\text{ }\mu\text{m}$  (Fig. 2(c)). There is no evidence of presence of  $\alpha$  as Fig. 2(d) shows.

The tensile properties of the alloy in solution treated conditions are listed in Table 2. The solution treated alloy has a moderate strength level with an excellent ductility. The alloy solution treated at  $775^{\circ}\text{C}$  exhibits higher strength but lower ductility than that at  $830^{\circ}\text{C}$ . The relatively higher strength can be attributed to the fine-grain strengthening of  $\beta$  grain which benefited from the primary  $\alpha$  phase [15]. The higher ductility in  $\beta$  solution treatment was also found in literature [15], but the reason for this is not clear.

#### 3.2. $\alpha/\beta$ solution treated plus aged conditions

The microstructures of the alloy along the transversal section after the  $\alpha/\beta$  solution treated at  $775^{\circ}\text{C}$  plus  $\alpha$  aged for 8 h are shown in Figs. 3. For  $\beta$  titanium alloys, the primary  $\alpha$  could limit the recrystallization and growth of  $\beta$  phase grains [23]. It is clearly to see that the primary  $\alpha$  distributes at grain boundary with the  $\beta$  grain size is only a few microns. It means that the primary  $\alpha$  has a distinctly pinning effect on growth of  $\beta$  grain in  $\alpha/\beta$  solution treated condition. During aging heat treatment, the secondary  $\alpha$  phase with an acicular shape was formed in the matrix. After aging at  $440^{\circ}\text{C}$  very smaller secondary  $\alpha$  phase was observed within matrix. Fig. 4 shows TEM image and  $[111]_{\beta}$  selected area diffraction pattern of the alloy aged at  $440^{\circ}\text{C}$ . It can be seen that the secondary  $\alpha$  phase distributed in matrix with nonuniform size and followed by a Burgers orientation relationship  $(0001)_{\alpha}/(110)_{\beta}$ ,  $[11\bar{2}0]_{\alpha}/[111]_{\beta}$  with  $\beta$  matrix. The size and volume fraction of secondary  $\alpha$  are strongly determined by the temperature. More

based on the SEM micrographs. TEM observation was performed on Philips-CM12. The TEM samples were machined to a diameter of 3.0 mm by electron discharge method and then polished into  $100\text{ }\mu\text{m}$  in thickness with 400–2000 grid SiC paper in water, and finally prepared with twin jet electrochemical polishing method.

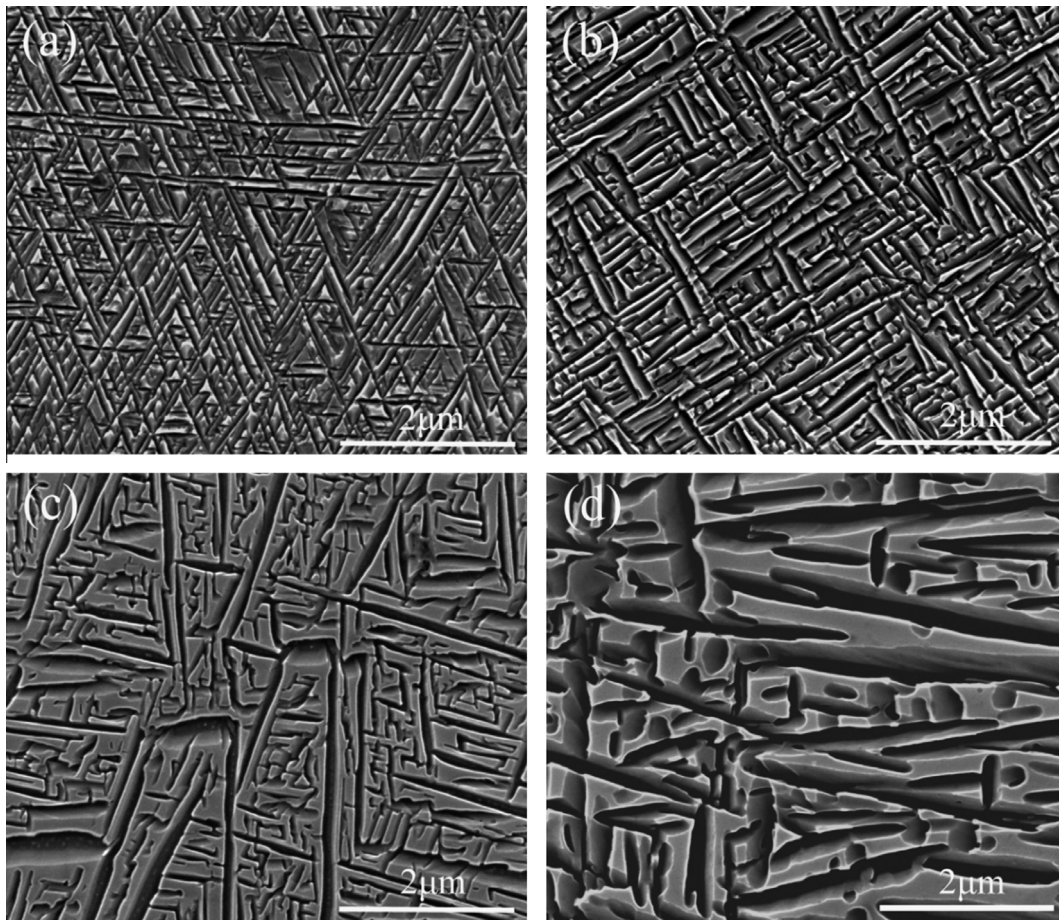


Fig. 8. Microstructures of the alloy along the transversal section solution treated at 830 °C and aged for 8 h at: (a) 440 °C, (b) 480 °C, (c) 520 °C and (d) 560 °C.

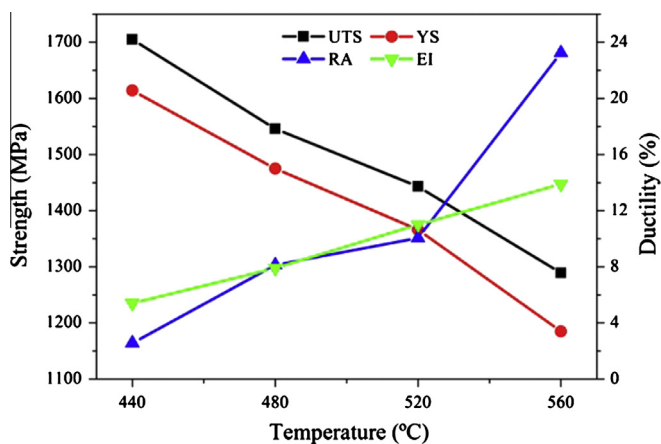


Fig. 9. Tensile properties of the alloy after solution treated at  $\beta$  field plus aged.

detailed microstructural measurements are shown in Figs. 5 and 6 that the volume fraction of total  $\alpha$  decreased from 61% after aging at 440 °C to 30% (primary  $\alpha$  is 5%) after aging at 560 °C, and the width of secondary  $\alpha$  increased from 0.028  $\mu\text{m}$  to 0.16  $\mu\text{m}$  simultaneously. The volume fraction decreased with increasing of temperature and the size of  $\alpha$  changed in the opposite way. This trend is because of the higher temperature will provide more driving force for growth but lower for nucleation of  $\alpha$ . Meanwhile, the  $\alpha$  phase also precipitated at grain boundaries and developed into a continuous film and it became coarser with increasing of aging

temperature. The tensile properties of the alloy after solution treated at 775 °C plus aged are shown in Fig. 7. It can be seen that the alloy has an excellent balance of strength and ductility. Especially aged at lower temperature (440 °C) the yield strength is 1624 MPa with a moderate elongation (6.2%). With increasing of aging temperature the strength of alloy decreased and the ductility increased. When aged at 560 °C the alloy has a greatest elongation (16.4%) with a moderate strength (1409 MPa). For every increase of 40 °C aging temperature, the yield strength is decreased by an average of 103 MPa. It means that the tensile properties of the alloy after  $\alpha/\beta$  solution treatment are very sensitive to aging temperature.

### 3.3. $\beta$ solution treated plus aged conditions

The microstructures of the alloy along the transversal section after the  $\beta$  solution treated plus aged are shown in Fig. 8. At lower aging temperature, the acicular secondary  $\alpha$  phase precipitated in the matrix. With increasing of aging temperature the variation of secondary  $\alpha$  is consistent with the trend that solution treated at  $\alpha/\beta$  region that the volume fraction of secondary  $\alpha$  decreased from 64% to 35% and the width of secondary  $\alpha$  increased from 0.042  $\mu\text{m}$  to 0.23  $\mu\text{m}$  (Figs. 5 and 6). It can be seen that the alloy has a higher volume fraction and larger size of secondary after solution treated at  $\beta$  field than at  $\alpha/\beta$  field. For  $\beta$  titanium alloy, solution treated at  $\beta$  region results in the least stable matrix composition and the greatest driving force for subsequent decomposition [24]. In this sense, the secondary  $\alpha$  will be easier to nucleate and growth and so bring out larger size for solution treated at  $\beta$  region. The tensile



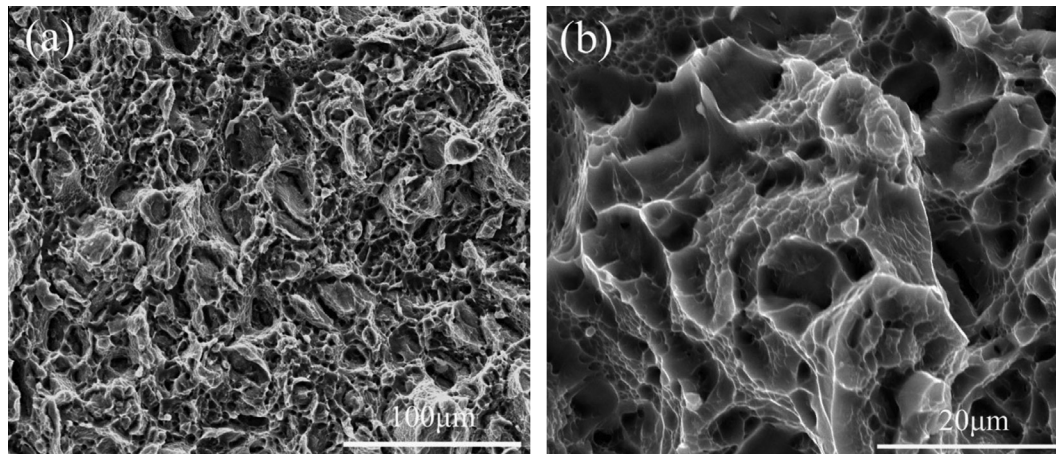


Fig. 10. SEM images of fracture surfaces of the alloy after solution treated at  $\alpha/\beta$  and aged at 480 °C for 8 h.

properties of the alloy after solution treated at 830 °C are shown in Fig. 9. Similar with the condition of solution treated at  $\alpha/\beta$  field plus aged that the strength of the alloy decreased and the ductility increased with the increase of aging temperature. At lower aging temperature (440 °C), the yield strength of alloy is 1619 MPa which is very close to condition of  $\alpha/\beta$  solution treated plus aged. But at higher temperatures (above 440 °C), the strength is much lower than  $\alpha/\beta$  solution treated plus aged condition. For every increase of 40 °C aging temperature, the yield strength is decreased by an average of 143 MPa.

#### 4. Discussion

Microstructures observation and tensile results show that the tensile properties of Ti–3.5Al–5Mo–6V–3Cr–2Sn–0.5Fe alloy are significantly influenced by the microstructures, especially the volume fraction and size of secondary  $\alpha$  phase. It can be seen that increased the aging temperature leads to a decrease in strength and an increase in ductility. This variation trend of strength is caused by the noticeable coarsening besides the volume fraction reducing of secondary  $\alpha$  phase with increasing of aging temperatures [15]. This result agreement with literature [12] that the yield strength is associated with the area fraction and the size of secondary  $\alpha$  phases, and the yield strength can be expressed by the following rule of mixture:

$$\sigma = \text{function of } (f\alpha_p 1/d\alpha_p + f\alpha_s 1/d\alpha_s) \quad (2)$$

where  $\sigma$  is the total yield strength,  $f\alpha_p$  is the area fraction of  $\alpha_p$  (primary  $\alpha$ ) phase, and  $f\alpha_s$  is the area of  $\alpha_s$  (secondary  $\alpha$ ) phase,  $d\alpha_p$  is the size of  $\alpha_p$ ,  $d\alpha_s$  is the size of  $\alpha_s$  phase.

In present work, either  $\alpha/\beta$  solution treatment or  $\beta$  solution treatment, tensile samples were solution treated at a constant temperature, so the volume fraction and the size of primary  $\alpha$  are constant. And the function can be written as follows:

$$\sigma = \text{function of } f\alpha_s 1/d\alpha_s \quad (3)$$

It can be seen that the increase of the volume fraction of secondary  $\alpha$  or decrease of the size of secondary  $\alpha$  will improve yield strength. In case of lower aging temperatures, the  $\alpha$  precipitates with a very small size is less than 50 nm in width lead to a quite high yield strength of 1624 MPa with an acceptable elongation of 6.2%. At higher aging temperatures, the  $\alpha$  phase coarsening with non-uniform size distribution results in a sharp reduction in strength.

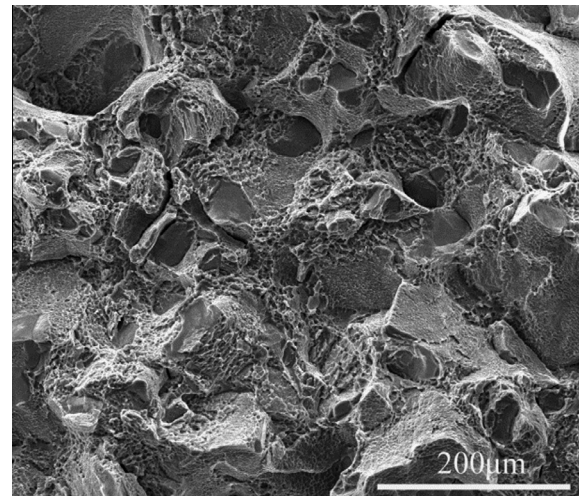
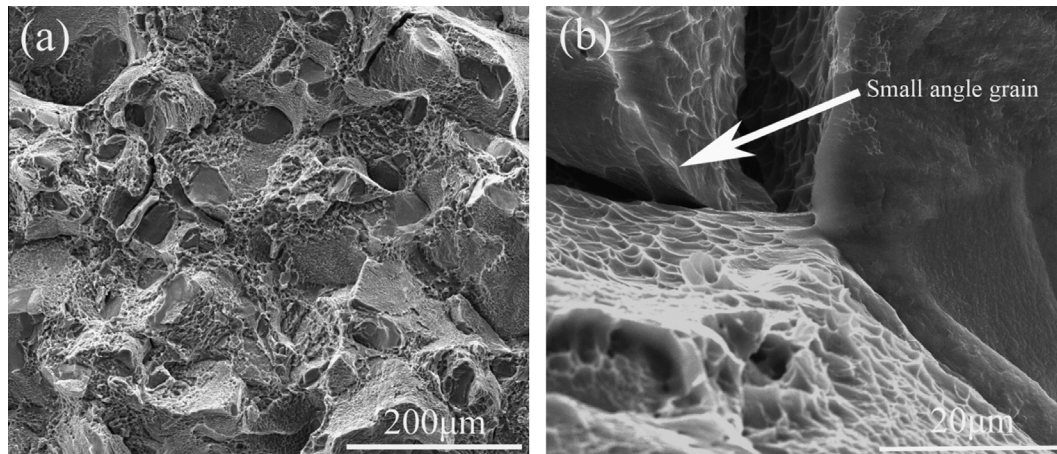


Fig. 11. SEM images of fracture surfaces of the alloy after solution treated at  $\beta$  and aged at 480 °C for 8 h.

One reasonable explanation of ductility improvement in  $\alpha/\beta$  solution treated plus aged condition should be the contribution of relatively small sized prior  $\beta$  grains. In the present study, the alloy shows a small grain size due to the limitation of primary  $\alpha$  phases (Fig. 3(a)) [24]. According to the Hall–Petch relationship that the small grain size is beneficial to the strength [25]. Moreover, a small grain size is also favored to tensile ductility, because the length of the  $\beta$  grain boundary will limit the maximum slip length possible in the  $\beta$  grain boundary  $\alpha$  layers. Moreover, a small grain size is also favored to tensile ductility. Because the tensile ductility is mainly determined by crack nucleation resistance which is strongly dependent on effective slip length parallel to the grain boundary  $\alpha$ -layers, and the small  $\beta$ -grain size of the bi-modal microstructure can greatly reduces the slip length and increasing crack nucleation resistance [14]. The dominant deformation mode for the  $\alpha/\beta$  solution treated plus aged condition is that the strain localization in matrix leading to voids at the interface between aged matrix and primary  $\alpha$  phase [13]. Fig. 10 shows the fracture surface of tensile sample after solution treated at  $\alpha/\beta$  region and aged. Lots of deep and fine ductile dimples in fracture surface of the specimen represented the excellent ductility of the alloy.



**Fig. 12.** Grain boundary triple point of alloy after solution treated plus aged and fractured (a) solution treated at 830 °C plus aged at 520 °C (b) after fractured.

Similar with solution treated at  $\alpha/\beta$  region plus aged condition that the strength of the alloy decreased and the ductility increased with the increase of aging temperature in  $\beta$  solution treated plus aged condition. This trend also can be explained by function (3). However, the strength of alloy which solution treated at single  $\beta$  region is more sensitive to aging temperature because of the yield strength is decreased by an average of 143 MPa for every increase of 40 °C. The reason for this difference can be explained by the larger size of secondary  $\alpha$  phase. As mentioned above, solution treated at  $\beta$  region results in the least stable matrix composition and the greatest driving force and leads to larger size of secondary  $\alpha$ . The lower ductility in  $\beta$  solution plus aged condition is caused by grain boundary  $\alpha$  and larger grain size. Fig. 11 shows the fracture surface of alloy solution treated at 830 °C plus aged at 520 °C for 8 h exhibits mainly intergranular fracture besides minor ductile fracture. The predominant parameter responsible for the low ductility is the grain boundary  $\alpha$  film in  $\beta$  solution treated microstructure (Fig. 12(a)). The presence of grain boundary  $\alpha$  film leads to long soft zones which deform preferentially during plastic deformation, and the high stress concentrations and high local strains develop at boundary triple points and results in separation of grains [13,14]. As the Fig. 12(b) shows, the local stress concentration at boundary triple points and leads to  $\beta$  grain separation. It is interesting to note that it seems that the separation developed at the small angle grain (white arrow). It is probably because the smaller angle grain at triple points will bear a larger load than other two grains. Although grain boundary  $\alpha$  film formed in bimodal microstructure and coarsen with increasing of aging temperature, but it did not reduce ductility. On the other hand, the small  $\beta$  grain size of the bimodal microstructure can reduce the slip length and increase crack nucleation resistance [14].

## 5. Conclusions

In this study, effect of microstructure characteristic on tensile properties of a new  $\beta$  high strength Ti–3.5Al–5Mo–6V–3Cr–2Sn–0.5Fe alloy was investigated systematically. The main results are summarized as follows:

- (1) In the Ti–3.5Al–5Mo–6V–3Cr–2Sn–0.5Fe alloy, the primary  $\alpha$  formed during solution treated slightly below  $\beta$  transus and leads to small grain size. Solution treatment slightly above  $\beta$  transus for a short time leads to dramatically growth of grains.
- (2) During aging treatments, the size and volume fraction of secondary  $\alpha$  are very sensitive to temperature. The volume

fraction decreased and the size increased with increasing of aging temperature. The size of secondary  $\alpha$  phase is larger than  $\alpha/\beta$  solution treatment plus aging condition for  $\beta$  solution treatment plus aging treatment.

- (3) The size and volume fraction of secondary  $\alpha$  affect the properties of the alloy strongly. When aged at 440 °C, the yield strength exceeds 1600 MPa both at  $\alpha/\beta$  and  $\beta$  solution treated plus aged conditions which the alloy have the highest volume fraction and the smallest size of secondary  $\alpha$  than aged at higher temperatures.
- (4) Grain boundary  $\alpha$  is responsible for the low ductility of  $\beta$  solution treatment plus aging treatment. The presence of grain boundary  $\alpha$  film leads to the high stress concentrations and high local strains developed at boundary triple points and resulted in separation of grains, and it seems that the separation happened at the small angle grain.

## References

- [1] Leyens C, Peters M. Titanium and Titanium Alloys. Weinheim: WILEY-VCH Verlag GmbH & Co. KGaA; 2003.
- [2] Boyer RR. Attributes, characteristics and application of titanium and its alloys. JOM 2010;62(5):21–4.
- [3] Nyakana SL, Fanning JC, Boyer RR. Quick reference guide for  $\beta$  titanium alloys in the 00s. J Mater Eng Perform 2005;14:799–811.
- [4] Boyer RR. Applications of beta titanium alloys in airframes. In: Eylon D, Boyer RR, Koss DA, editors. Beta titanium alloys in the 1990's. Pennsylvania (Warrendale): TMS; 1993. p. 335–46.
- [5] Fanning JC, Fox SP. Recent developments in metastable  $\beta$  strip alloys. J Mater Eng Perform 2005;14:703–8.
- [6] Sukumar G, Singh BB, Bhattacharjee A, Kumar KS, Gogia AK. Ballistic impact behaviour of  $\beta$ -CEZ Ti alloy against 7.62 mm armour piercing projectiles. Int J Impact Eng 2013;54:149–60.
- [7] Boyer RR, Briggs RD. The use of  $\beta$  titanium alloys in the aerospace industry. J Mater Eng Perform 2005;14:681–5.
- [8] Bania PJ. Beta titanium alloys and their role in the titanium industry. JOM 1994;46:16–9.
- [9] Srinivasu G, Natraj Y, Bhattacharjee A, Nandy TK, Nageswara Rao GVS. Tensile and fracture toughness of high strength  $\beta$  Titanium alloy, Ti–10V–2Fe–3Al, as a function of rolling and solution treatment temperatures. Mater Des 2013;47:323–30.
- [10] Boyer RR. Titanium for aerospace Rationale and applications. Adv Perform Mater 1995;2:349–68.
- [11] Hamajima T, Lütjering G, Weissmann S. Importance of slip mode for dispersion-hardened  $\beta$ -titanium alloys. Metall Mater Trans B 1973;4:847–56.
- [12] Mora L, Quesne C, Penelle R. Relationships among thermomechanical treatments, microstructure, and tensile properties of a near beta-titanium alloy:  $\beta$ -CEZ: Part II. Relationships between thermomechanical treatments and tensile properties. J Mater Res 1996;11:89–99.
- [13] Terlinde GT, Duerig TW, Williams JC. Microstructure, tensile deformation, and fracture in aged Ti–0V–2Fe–3Al. Metall Trans A 1983;14A:2101–15.
- [14] Sauer C, Lütjering G. Influence of  $\alpha$  layers at  $\beta$  grain boundaries on mechanical properties of Ti-alloys. Mater Sci Eng A 2001;319–321:393–7.

- [15] Li CL, Mi XJ, Ye WJ, Hui SX, Yu Y, Wang WQ. A study on the microstructures and tensile properties of new beta high strength titanium alloy. *J Alloy Compd* 2013;550:23–30.
- [16] Lütjering G. Influence of processing on microstructure and mechanical properties of ( $\alpha$  +  $\beta$ ) titanium alloys. *Mater Sci Eng A* 1998;243:32–45.
- [17] Bhattacharjee A, Joshi Vydehi A, Hussain SM, Gogia AK. Effect of thermomechanical processing on evolution of  $\alpha$  phase morphology in  $\beta$  titanium alloys. In: Gorynin IV, Ushkov SS, editors. *Titanium 99: science and technology*, vol. I. St. Petersburg, CRISM, Prometey; 2000. p. 164–171.
- [18] Weiss I, Froes FH, Eylon D, Welsch GE. Modification of alpha morphology in Ti–6Al–4V by thermomechanical processing. *Metall Trans A* 1986;17: 1935–47.
- [19] Ding R, Guo ZX, Wilson A. Microstructure evolution of a Ti–6Al–4V alloy during thermo-mechanical processing. *Mater Sci Eng A* 2002;A327: 233–45.
- [20] Margolin H, Cohen P. Evolution of the equiaxed morphology of phases in Ti–6Al–4V. In: Kimura H, Izumi O, editors. *Titanium 80: science and technology*. Japan: Kyoto; May 1980. p. 1555–61.
- [21] Margolin H, Cohen P. Kinetics of evolution of alpha in Ti–6Al–4V. In: Kimura H, Izumi O, editors. *Titanium 80: science and technology*. Kyoto, Japan; May 1980. p. 2991–1997.
- [22] Xu B, Wang XY, Zhou JK, Wang KX, Zeng WD. Microstructure evolvement regularity of TC17 titanium alloy in hot deformation. *Trans Nonferrous Met Soc China* 2010;20:167–72.
- [23] Duerig TW, Terlinde GT, Williams JC. Phase transformations and tensile properties of Ti–10V–2Fe–3Al. *Metall Trans A* 1980;11:1987–98.
- [24] Duerig TW, Williams JC. In: Boyer RR, Rosenberg HW, editors. *Beta-titanium alloys in the 1980's*, 1984. p. 19–69.
- [25] Petch NJ. The cleavage strength of polycrystals. *J Iron Steel Inst* 1953;174:25–8.